RESEARCH PAPER

Formulation Development and In Vivo Evaluation of Syzygium aromaticum Extract-Loaded Microspheres for Neuroprotective Activity

Virashri Dhumal[1]*, Sushila Kaura[2]

[1*,2] *Department of Pharmaceutical Sciences, Jayoti Vidyapeeth Women's University, Jaipur-303122, Rajasthan, India*

ABSTRACT

Objectives: To develop and optimize Syzygium aromaticum extract-loaded microspheres using Box-Behnken design and evaluate their neuroprotective efficacy in rotenone-induced Parkinson's disease model for potential clinical translation in neurodegenerative disorder management. Methods: Syzygium aromaticum ethanolic extract was prepared by Soxhlet extraction and characterized for physicochemical properties. Microspheres were formulated using oil-in-water emulsion-solvent evaporation method and optimized through Box-Behnken design with sodium alginate concentration, Tween 80 concentration, and stirring speed as independent variables. Seventeen formulations were prepared and evaluated for particle size, entrapment efficiency, drug release, and stability. The optimized batch (F14) was selected based on desirability function demonstrating optimal particle size and maximum entrapment efficiency. Neuroprotective efficacy was assessed in Swiss albino mice using rotenone-induced Parkinson's model through behavioral tests (rotarod, catalepsy, open field, actophotometer) and biochemical estimations (CAT, GSH, SOD, MDA). Results: The optimized formulation F14 exhibited particle size of 378.64±16.15 µm, entrapment efficiency of 83.66±3.35%, and sustained release of 89.92±4.68% over 12 hours. In vivo studies demonstrated superior neuroprotection with microsphere formulation significantly improving motor coordination (144.3±13.9 sec), reducing catalepsy (33.8±5.9 sec), enhancing locomotor activity (146.5±12.8 counts), and restoring antioxidant enzymes (catalase: 11.25±1.3 µM/mg protein/min; GSH: 10.95±1.3 nM/mg protein) compared to pure extract ($p<0.05$-0.001). Conclusion: The developed microsphere formulation demonstrated enhanced neuroprotective efficacy through improved bioavailability and sustained release, offering significant clinical potential for neurodegenerative disease management. These findings provide strong rationale for advancing this formulation toward preclinical toxicity studies and clinical trials.

Keywords: Syzygium aromaticum; Microspheres; Box-Behnken design; Neuroprotection; Parkinson's disease; Rotenone; Antioxidant activity.

How to cite this article: Dhumal V, Kaura S.. Formulation Development and In Vivo Evaluation of Syzygium aromaticum Extract-Loaded Microspheres for Neuroprotective Activity Int J Drug Deliv Technol. 2026;16(6s): 30-50; DOI: 10.25258/ijddt.16.6s.4

Source of support: Nil.

Conflict of interest: None

INTRODUCTION

Neurodegenerative disorders, including Alzheimer's disease, Parkinson's disease, and other cognitive impairments, represent a significant global health challenge affecting over 50 million people worldwide.[1] The prevalence of these conditions is projected to triple by 2050, creating an unprecedented burden on healthcare systems and economies.[2] Current therapeutic approaches remain largely symptomatic, with limited disease-modifying treatments available. Conventional pharmacological interventions face substantial challenges including poor blood-brain barrier penetration, rapid systemic clearance, and significant adverse effects. The economic burden exceeds $800 billion annually, encompassing direct medical costs and indirect caregiving expenses.[3] Recent trends highlight an urgent need for novel neuroprotective agents derived from natural sources, combined with advanced delivery systems that can overcome biological barriers. The inadequacy of existing treatments, coupled with the progressive and irreversible nature of neurodegeneration, necessitates innovative therapeutic strategies that address both efficacy and delivery limitations while minimizing toxicity.[4]

Syzygium aromaticum, commonly known as clove, represents a promising natural source of neuroprotective compounds, with eugenol constituting 70-90% of its essential oil composition. This phenylpropanoid compound exhibits remarkable antioxidant, anti-inflammatory, and neuroprotective properties through multiple mechanisms including free radical scavenging, inhibition of lipid peroxidation, and modulation of inflammatory cytokines.[5] The extract demonstrates significant ability to attenuate oxidative stress-induced neuronal damage by upregulating endogenous antioxidant enzymes and suppressing pro-apoptotic pathways. Previous investigations have established its efficacy in ameliorating cognitive deficits in various experimental models, attributed to its capacity to inhibit acetylcholinesterase activity and reduce amyloid-beta aggregation.[6] The polyphenolic constituents possess metal-chelating properties that prevent iron-catalyzed oxidative reactions implicated in neurodegeneration. Despite these therapeutic advantages, the clinical translation of *Syzygium aromaticum* extract faces substantial limitations including poor aqueous solubility, rapid metabolism, and limited bioavailability in the central nervous system. These pharmacokinetic

**Author for Correspondence: dhumalvirashri790@gmail.com*

challenges significantly compromise its therapeutic potential, necessitating innovative formulation approaches.[7] Microspheres have emerged as superior drug delivery platforms, offering unique advantages for encapsulating and delivering bioactive compounds across biological barriers. These microcarriers possess spherical polymeric structures with excellent drug loading capacity and controlled release characteristics.[8] The exceptional biocompatibility, large surface area, and ease of surface functionalization make them ideal candidates for brain-targeted delivery. Recent advances demonstrate their ability to enhance blood-brain barrier penetration through receptor-mediated transcytosis and passive diffusion mechanisms.[9] The functional groups on the surface facilitate conjugation with targeting ligands, enabling site-specific delivery while minimizing off-target effects. Microspheres provide protection against enzymatic degradation and premature clearance, significantly improving the pharmacokinetic profile of encapsulated therapeutics. Their microscale dimensions facilitate cellular uptake through endocytic pathways, ensuring intracellular delivery of therapeutic agents. Furthermore, these systems exhibit pH-responsive release characteristics, enabling preferential drug release in pathological microenvironments. The biocompatible polymeric framework undergoes gradual biodegradation, eliminating concerns regarding long-term accumulation and systemic toxicity.[9]

The present study aims to develop and characterize *Syzygium aromaticum* extract-loaded microspheres and evaluate their neuroprotective efficacy through comprehensive in vivo investigations. Specific objectives include optimization of formulation parameters, physicochemical characterization, assessment of blood-brain barrier penetration, and evaluation of neuroprotective activity in experimental animal models. This research addresses critical gaps in natural product delivery for neurodegenerative disorders.

MATERIALS AND METHODS

MATERIALS

Sodium alginate (pharmaceutical grade), Tween 80 (polysorbate 80), and dichloromethane (DCM, 99.5%, analytical grade) Research Lab Fine Chem Industries, Mumbai, India. Calcium chloride ($CaCl_2$, 97%, analytical grade) Loba Chemie Pvt. Ltd., Mumbai, India. Ethanol (99.9%, HPLC grade), methanol (99.8%), and glacial acetic acid Merck Life Science Pvt. Ltd., Mumbai, India. Sodium hydroxide (98%), hydrochloric acid (37% w/v), and phosphate buffer salts (pH 1.2 and 7.4) SD Fine-Chem Ltd., Mumbai, India. Sodium carboxymethyl cellulose (Na-CMC), rotenone (≥95%, analytical grade), and standard levodopa Sigma-Aldrich (Merck), Bangalore, India. All other chemicals and reagents used were of analytical grade. Double-distilled water was used throughout the study.

METHODS

Plant Material

Dried flower buds of *Syzygium aromaticum* (L.) was procured from an authenticated herbal vendor in Pune, Maharashtra, India. The plant material was authenticated (BSI/WRC/Tech./2024/JVD-50) at the Botanical Survey of India, Western Regional Centre, Koregaon Park, Pune-411001. The authenticated material was thoroughly washed with distilled water, shade-dried at room temperature (25±2°C), coarsely powdered using a mechanical grinder, passed through sieve No. 40, and stored in airtight amber-colored glass containers until further use.[10,11]

Preparation of Extract

The dried and powdered flower buds of *Syzygium aromaticum* (100 g) were subjected to Soxhlet extraction using ethanol (95% v/v, 500 mL) as the extraction solvent. The extraction was carried out at 60-70°C for 6-8 hours until the solvent in the siphon tube became colorless, indicating complete extraction. The ethanolic extract was filtered through Whatman filter paper No. 1, and the filtrate was concentrated under reduced pressure using a rotary evaporator (Buchi Rotavapor R-210, Switzerland) at 45°C. The concentrated extract was further dried in a vacuum desiccator to remove residual solvent traces and obtain a dark brown semi-solid extract. The percentage yield was calculated based on the dry weight of the extract obtained relative to the initial weight of plant material used. The dried extract was stored in an airtight amber-colored glass container in a refrigerator at 4°C until further use for phytochemical analysis and formulation development.[12,13]

Determination of Scanning Absorbance Maxima

The wavelength of maximum absorbance (λ_{max}) for *Syzygium aromaticum* extract (SAE) was determined using UV-Visible spectrophotometry. Stock solution was prepared by dissolving 10 mg of extract in 10 mL of methanol (1000 µg/mL). Working solution (10 µg/mL) was prepared by appropriate dilution with methanol and scanned in the UV-visible range of 200-800 nm against methanol as blank. The wavelength showing maximum absorbance was recorded as λ_{max} and used for all further spectrophotometric analyses and quantification studies.[14]

Preparation of Calibration Curve

Standard calibration curve for SAE was prepared to establish linearity between concentration and absorbance. From the stock solution (1000 µg/mL), working standard solutions of 5, 10, 15, 20, 25, and 30 µg/mL were prepared by dilution with methanol. The absorbance of each concentration was measured at λ_{max} against methanol as blank. Calibration curve was plotted with concentration on x-axis and absorbance on y-axis. The linearity was assessed by calculating correlation coefficient (R^2), and regression equation was determined for quantification purposes in subsequent analytical studies.[15,16]

Solubility Studies

The solubility of SAE was determined by solvent saturation method. Excess amount of extract was added to 10 mL of different solvents including water, methanol, ethanol, acetone, chloroform, and dichloromethane in separate stoppered conical flasks. Mixtures were mechanically shaken at 25±2°C for 24 hours, allowed to stand for 2 hours, and filtered through Whatman filter paper No. 41. The concentration of dissolved extract was determined spectrophotometrically at λ_{max} using calibration curves. Solubility was expressed as mg/mL for each solvent.[17]

Determination of Melting Point

The melting point of SAE was determined using capillary tube method. Dried extract was finely powdered and filled into clean, dry capillary tubes. The capillary tubes were placed in melting point apparatus, and temperature was gradually increased at 1-2°C per minute. The initial and final melting temperatures were recorded. Measurements were performed in triplicate to ensure reproducibility.[18]

Differential Scanning Calorimetry (DSC)

DSC studies were performed to investigate thermal behavior and compatibility of SAE with formulation excipients. Accurately weighed samples (2-5 mg) of pure extract and physical mixtures with excipients (1:1 ratio) were placed in sealed aluminum pans. Samples were heated at 10°C/min over 30-300°C under nitrogen atmosphere (50 mL/min flow rate) using empty sealed aluminum pan as reference. Thermograms were analyzed for characteristic peaks, melting points, and thermal behavior changes to assess drug-excipient compatibility.[19]

Fourier Transform Infrared Spectroscopy (FTIR)

FTIR was performed to identify characteristic functional groups in SAE and study compatibility with formulation excipients. Samples were prepared using KBr pellet method, wherein 2-3 mg of pure extract or physical mixture was mixed with 100 mg of dried KBr powder and compressed under hydraulic pressure. FTIR spectra were recorded in 4000-400 cm^{-1} range with 4 cm^{-1} resolution. Characteristic peaks were identified and analyzed. Any shift, appearance, or disappearance of peaks in physical mixtures compared to pure extract was examined to assess interactions and confirm formulation compatibility.[20]

Experimental Design

A Box-Behnken Design (BBD) was employed to optimize the microsphere formulation. Independent variables were sodium alginate concentration (X_1), Tween 80 concentration (X_2), and stirring speed (X_3). Dependent variables were particle size (Y_1) and entrapment efficiency (Y_2). The design consisted of 17 experimental runs including 12 factorial points and 5 center points. Experimental data was fitted to a second-order polynomial equation:

$$Y = \beta_0 + \beta_1X_1 + \beta_2X_2 + \beta_3X_3 + \beta_{12}X_1X_2 + \beta_{13}X_1X_3 + \beta_{23}X_2X_3 + \beta_{11}X_1^2 + \beta_{22}X_2^2 + \beta_{33}X_3^2$$

Statistical analysis including ANOVA, regression analysis, and response surface plots were performed using Design-Expert® software (Version 13, Stat-Ease Inc., Minneapolis, USA). Model adequacy was assessed using R^2, adjusted R^2, predicted R^2, and adequate precision values.[21,22]

Table 1: Independent and Dependent Variables with Their Levels Used in Box-Behnken Design for Microsphere Optimization

Independent Variables	**Levels**	
	Low level (-1)	**High Level (+1)**
Sodium Alginate (% w/v)	1	3
Tween 80 (% v/v)	0.5	1
Stirring Speed (rpm)	800	1200
Dependent Variables		
Particle Size **(µm)**		Minimize
Entrapment Efficiency (%)		Maximize

Formulation of Microspheres

Syzygium aromaticum extract-loaded microspheres (SA-Microspheres) were prepared by oil-in-water emulsion-solvent evaporation method. Sodium alginate (1.0-3.0% w/v) was dissolved in a mixture of dichloromethane and ethanol (2:1 v/v, 30 mL total) under magnetic stirring for 1-2 hours. *SAE* was incorporated in a polymer to extract ratio of 1:5 (w/w) and stirred for 30 minutes. This organic phase was added dropwise into aqueous phase containing distilled water (200 mL) with Tween 80 (0.5-1.0% v/v) and stirred at controlled speeds (800-1200 rpm) for 3-4 hours to allow solvent evaporation. The microspheres were cross-linked by adding calcium chloride solution (5% w/v, 20 mL) dropwise under continuous stirring for 30 minutes. Microspheres were separated by filtration, washed thoroughly with distilled water (5×50 mL), dried at 40±2°C for 24 hours, and stored in airtight amber-colored glass containers in a desiccator until further use. All formulations were prepared in triplicate according to Box-Behnken Design matrix, and particle size (Y_1) and entrapment efficiency (Y_2) were evaluated for each batch.[23,24]

Table 2: Formulation Composition of Herbal Microspheres According to Box-Behnken Design

Batch Code	Sodium Alginate (% w/v)	Tween 80 (% v/v)	*Herbal Extract (% w/v)**	DCM (mL)	Ethanol (mL)	Distilled Water (mL)	$CaCl_2$ 5% w/v (mL)
F1	1.0	1.0	0.2	20	10	200	20
F2	2.0	1.0	0.4	20	10	200	20
F3	1.0	0.75	0.2	20	10	200	20
F4	2.0	0.75	0.4	20	10	200	20
F5	2.0	0.75	0.4	20	10	200	20
F6	2.0	0.75	0.4	20	10	200	20
F7	2.0	0.75	0.4	20	10	200	20
F8	3.0	0.5	0.6	20	10	200	20
F9	2.0	1.0	0.4	20	10	200	20
F10	2.0	0.5	0.4	20	10	200	20
F11	1.0	1.0	0.2	20	10	200	20
F12	2.0	0.75	0.4	20	10	200	20
F13	2.0	0.5	0.4	20	10	200	20
F14	3.0	0.75	0.6	20	10	200	20
F15	3.0	1.0	0.6	20	10	200	20
F16	1.0	0.5	0.2	20	10	200	20
F17	3.0	0.75	0.6	20	10	200	20

Characterization of Microspheres

Percentage Yield

The percentage yield of SA-Microspheres was calculated to assess formulation efficiency. Dried microspheres from each batch were accurately weighed using a digital analytical balance (Sartorius, Germany). Percentage yield was calculated using:

Percentage Yield (%) = (Practical mass of microspheres / Theoretical mass of microspheres) × 100

All measurements were performed in triplicate, and results were expressed as mean ± S.D.[25]

Particle Size and Particle Size Distribution

Mean particle size and distribution were determined using dynamic light scattering (DLS). Microspheres were dispersed in distilled water at 0.1 mg/mL and analyzed using a Zetasizer Nano ZS (Malvern Instruments, UK) at 25 ± 0.5°C. Mean particle size, polydispersity index (PDI), and size distribution were calculated. All measurements were performed in triplicate, and results were expressed as mean ± S.D.[26]

Zeta Potential Determination

Zeta potential was measured to assess surface charge and predict physical stability. Microspheres were dispersed in distilled water (pH 7.0) at 1 mg/mL and subjected to probe ultrasonication at 40% amplitude for 5 minutes. Zeta potential was determined using Zetasizer Nano ZS at 25±0.5°C. Measurements were performed with at least 15 runs in triplicate and expressed as mean ± S.D. Values greater than ±30 mV indicate excellent stability, ±20 to ±30 mV indicate good stability, and below ±20 mV suggest potential aggregation.[27]

Drug Loading and Entrapment Efficiency

Drug Loading (DL%)

Accurately weighed microspheres (50 mg) were crushed and transferred to a 100 mL volumetric flask containing methanol, vortexed for 10 minutes, and kept at room temperature for 24 hours with intermittent shaking. The solution was filtered through Whatman filter paper No. 41, diluted, and analyzed spectrophotometrically at λ_{max} using UV-Vis spectrophotometer (Shimadzu UV-1800, Japan). Drug loading was calculated using:

Drug Loading (%) = (Actual drug content / Weight of microspheres) × 100

Entrapment Efficiency (EE%)

Accurately weighed microspheres (50 mg) were crushed and transferred to a 250 mL volumetric flask containing PBS (pH 7.4). The flask was kept at 37±0.5°C for 24 hours with occasional shaking, stirred at 500 rpm for 20 minutes, and filtered through Whatman filter paper No. 40. The extract amount was determined spectrophotometrically at λ_{max}. Entrapment efficiency was calculated using:

Entrapment Efficiency (%) = (Actual drug content / Theoretical drug content) × 100

All measurements were performed in triplicate, and results were expressed as mean ± S.D.[28,29]

In Vitro Drug Release Studies

In vitro release profile was evaluated using USP Type-II dissolution apparatus (Electrolab TDT-08L, Mumbai, India). Microspheres equivalent to 10 mg extract were

placed in 900 mL of 0.1 N HCl (pH 1.2) at 37±0.5°C with 50 rpm paddle speed for 2 hours to simulate gastric conditions, then replaced with PBS (pH 7.4) for up to 12 hours. At predetermined intervals (0.5, 1, 2, 3, 4, 6, 8, 10, and 12 h), 5 mL aliquots were withdrawn and replaced with fresh buffer. Samples were filtered through 0.45 µm PVDF filters and analyzed spectrophotometrically at λ_{max}. Cumulative percentage drug release was calculated using:

Cumulative % Drug Release = (Ct × V + Σ Ci × S) / Total drug content × 100

where Ct is concentration at time t, V is volume of dissolution medium, Ci is concentration of withdrawn sample, and S is sample volume. All experiments were performed in triplicate, and results were expressed as mean ± S.D. Release data was fitted to zero-order, first-order, Higuchi, Korsmeyer-Peppas, and Hixson-Crowell models to determine release mechanism.[30]

Morphological Analysis by Scanning Electron Microscopy (SEM)

Surface morphology and texture of optimized SA-Microspheres were examined using SEM (JEOL JSM-6510LV, Japan). Microspheres were mounted on aluminum stubs with double-sided carbon tape and sputter-coated with gold-palladium alloy for 120 seconds. Samples were examined at 15-20 kV accelerating voltage with varying magnifications (×100, ×500, ×1000, ×5000). Photomicrographs were captured to assess surface characteristics, particle uniformity, sphericity, surface texture, pores, and agglomeration.[31]

Stability Studies

Stability studies were conducted according to ICH Q1A (R2) guidelines. Optimized microsphere formulations were packed in amber-colored Type III glass vials with rubber stoppers and stored at long-term conditions (25±2°C / 60±5% RH) and accelerated conditions (40±2°C / 75±5% RH) in stability chambers. Samples were withdrawn at 0, 1, 2, 3, and 6 months and evaluated for physical appearance, particle size, drug content, entrapment efficiency, and in vitro drug release profile. Stability data was statistically analyzed using one-way ANOVA.[32]

Neuroprotective Activity

Experimental Animals

Male Swiss albino mice weighing 25-30 g were procured from the institutional animal house. Animals were maintained under standard laboratory conditions (25±2°C, 55±5% RH, 12-hour light/dark cycle) with free access to standard pellet diet and water ad libitum. All experimental procedures adhered to CCSEA protocols, Government of India. Approval (IIRT/IAEC/34/2025/012) was obtained from the Institutional Animal Ethical Committee before commencing experiments.

Rotenone-Induced Parkinson's Disease Model

Animals were randomly allocated into five experimental groups (n = 6). Group G1 (normal control) received the vehicle (distilled water), and Group G2 (disease control) received 0.5% w/v Na-CMC. Group G3 was treated with *Syzygium aromaticum* extract (SAE, 200 mg/kg), Group G4 received the optimized SA-microsphere formulation (SAMS- 200 mg/kg), and Group G5 was treated with levodopa and carbidopa (65 mg/kg and 20 mg/kg, respectively). Groups G2–G5 were induced with subcutaneous injections of rotenone (2.5 mg/kg in DMSO) on alternate days until day 21. All treatments were administered orally once daily throughout the study period. Neurobehavioral performance was assessed weekly up to day 21. On day 22, the animals were humanely sacrificed, and brain samples were isolated and analyzed for biochemical parameters.[33-34]

Behavioral Tests

Mice were acclimatized and trained for seven days before experimental protocol. Motor coordination and grip strength were assessed using rotarod test, cataleptic behavior using catalepsy test, and locomotor activity using open field test and actophotometer. All tests were conducted weekly for three consecutive weeks.[35]

Rotarod Test

Animals were placed on a rotating rod (3 cm diameter) at 20 rpm. Three test trials were conducted with 5-minute inter-trial intervals. Duration on the rotating rod was recorded as motor coordination index with 300-second cut-off time.[36]

Catalepsy Test

Each mouse was positioned with hind limbs on an elevated platform and forepaws on the floor. Latency to correct posture was recorded as catalepsy index. Test was repeated six times, and mean latency was calculated.[37]

Actophotometer Test

Animals were placed in actophotometer chamber and acclimatized for 60 seconds. Light beam interruptions by movements were recorded for 300 seconds. Locomotor activity was expressed as total photo-beam counts over 5 minutes[38]

Open Field Test

Animals were placed in square arena (100 cm × 100 cm × 40 cm) divided into 25 squares. Line crossings (all four paws in new square), total immobility time, and rearing behavior frequency were recorded for 300 seconds per animal.[39]

Preparation of Brain Homogenate

On day 22, animals were euthanized by cervical dislocation. Brains were rapidly excised, washed with ice-cold PBS (pH 7.4), and weighed. Whole brain tissue was homogenized (10% w/v) in ice-cold phosphate buffer (0.1 M, pH 7.4) on ice. Homogenate was

centrifuged at 10,000 rpm for 15 minutes at 4°C, and supernatant was collected for biochemical analyses.[40]

Estimation of Biochemical Parameters

Antioxidant enzymes including superoxide dismutase (SOD), catalase (CAT), reduced glutathione (GSH), and lipid peroxidation marker malondialdehyde (MDA) were estimated. Catalase activity was determined by measuring hydrogen peroxide decomposition at 240 nm. SOD activity was assessed by pyrogallol auto-oxidation inhibition method. GSH levels were estimated using Ellman's reagent (DTNB) at 412 nm. Lipid peroxidation was quantified by measuring TBARS as MDA equivalents at 532 nm.[41]

Statistical Analysis

Data are expressed as mean ± SD (n=6). Statistical analyses were performed using GraphPad Prism software (Version 10.0). One-way or two-way ANOVA followed by Tukey's or Bonferroni's post hoc test were applied. Values of *p<0.05, **p<0.01, and ***p<0.001 were considered significantly different compared with disease control. Values of #p<0.05 indicate significant differences compared with normal control, while Ψp<0.05 denotes significant differences compared with extract-treated groups (SAE).[42]

RESULTS

Calibration Curve Determination

The calibration curve of SAE demonstrated excellent linearity at 278 nm wavelength across the concentration range of 5-30 µg/mL. The linear regression analysis yielded a high correlation coefficient (R^2 = 0.9996), indicating strong proportional relationship between absorbance and concentration. The regression equation (y = 0.034x + 0.0078) with slope 0.034 and intercept 0.0078 was obtained and utilized for accurate quantification of extract content in subsequent analytical procedures including drug loading, entrapment efficiency, and in vitro release studies, ensuring reliable spectrophotometric determination throughout the investigation.

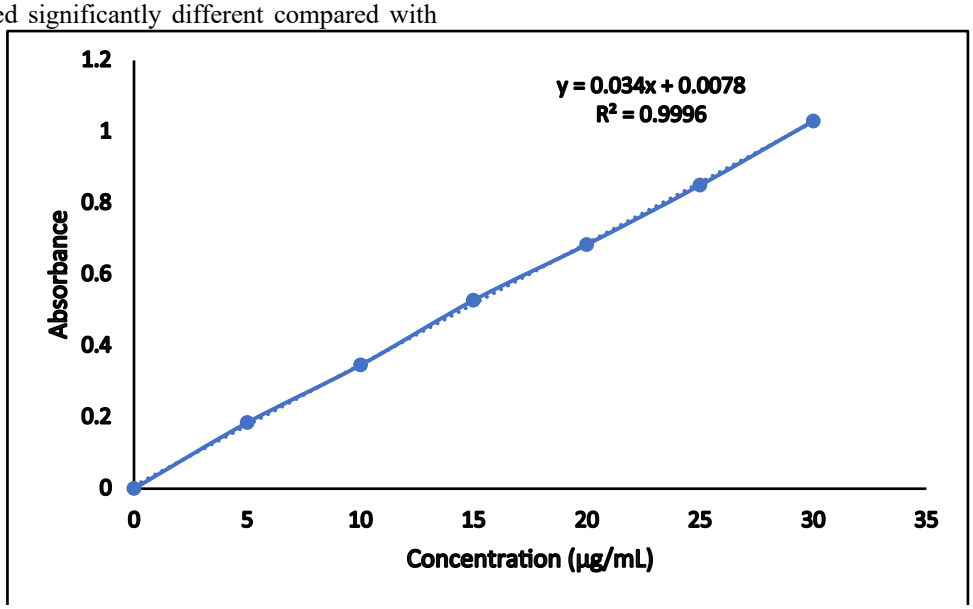

Figure 1: Calibration Curve of SAE at 278 nm

Solubility Study

The solubility profile of SAE revealed maximum solubility in ethanol (194.88±4.45 mg/mL) and methanol (186.25±3.17 mg/mL), classified as freely soluble. Moderate solubility was observed in chloroform (77.66±1.31 mg/mL) and acetone (68.45±1.53 mg/mL). The extract exhibited poor aqueous solubility in water (8.68±0.25 mg/mL) and phosphate buffer pH 7.4 (18.38±0.49 mg/mL), while petroleum ether showed minimal dissolution (0.50±0.07 mg/mL). These findings confirmed the lipophilic nature of the extract, justifying microencapsulation for enhanced bioavailability.

Table 2: Solubility Profile of SAE in Different Solvents

Sr. No.	Solvent	Solubility (mg/mL)	Inference
1	Water	8.68 ± 0.25	Slightly soluble
2	Methanol	186.25 ± 3.17	Freely soluble
3	Ethanol	194.88 ± 4.45	Freely soluble
4	Chloroform	77.66 ± 1.31	Soluble
5	Acetone	68.45 ± 1.53	Soluble
6	Petroleum Ether	0.50 ± 0.07	Very slightly soluble
7	Phosphate Buffer pH 7.4	18.38 ± 0.49	Sparingly soluble

Values are expressed as mean ± S.D. (n=3)

Melting Point Determination

The melting point determination of SAE was performed using capillary tube method, revealing a melting point of 59.2±1.8°C. This relatively low melting point indicates the semi-solid nature of the extract at room temperature, attributed to the presence of eugenol and other volatile phenolic compounds as major constituents. The narrow standard deviation (±1.8°C) demonstrated good reproducibility of measurements. This thermal characteristic was crucial for selecting appropriate processing conditions during microsphere formulation and provided baseline data for subsequent differential scanning calorimetry and thermogravimetric analyses.

Table 3: Melting Point of SAE

Sr. No.	Sample	Melting Point (°C)
1	*Syzygium aromaticum* Ethanolic Extract (SAE)	59.2 ± 1.8

Values are expressed as mean ± S.D. (n=3)

DSC Analysis

The DSC thermogram of *SAE* exhibited a characteristic sharp endothermic peak at 59.22°C, corresponding to its melting point and confirming the extract's thermal behavior. The physical mixture of extract with microspheres excipients displayed two distinct endothermic peaks at 59.16°C and 189.25°C. The preservation of the extract's characteristic peak at 59.16°C with minimal shift indicated absence of significant chemical interactions between the extract and formulation components. This compatibility confirmation was essential for proceeding with microsphere formulation, ensuring extract stability during processing and storage.

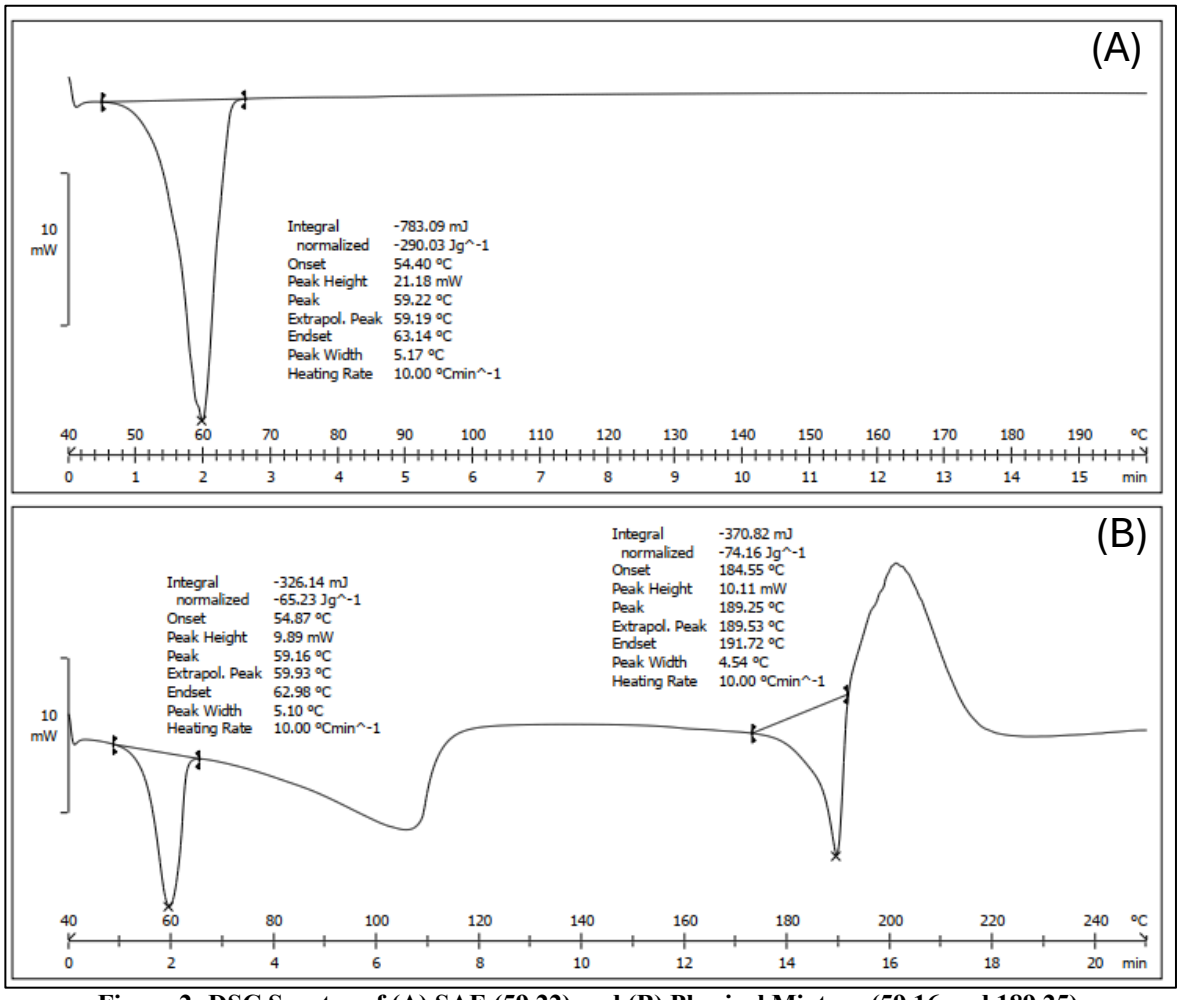

Figure 2: DSC Spectra of (A) SAE (59.22) and (B) Physical Mixture (59.16 and 189.25)

FTIR Analysis

The FTIR spectrum of *SAE* displayed characteristic peaks at 3410 cm^{-1} (O-H stretching), 3071 and 3009 cm^{-1} (aromatic C-H stretching), 2965, 2935, and 2853 cm^{-1} (aliphatic C-H stretching), 1632 cm^{-1} (asymmetric COO^- stretching), 1593 and 1514 cm^{-1} (aromatic C=C stretching), and 1278 and 1237 cm^{-1} (C-O stretching), confirming the presence of eugenol and phenolic compounds. The physical mixture exhibited minimal peak shifts with retention of major functional groups at 3413, 3046, 1514, and 1235 cm^{-1}, indicating no significant chemical interactions between extract and excipients, thereby confirming compatibility for formulation development.

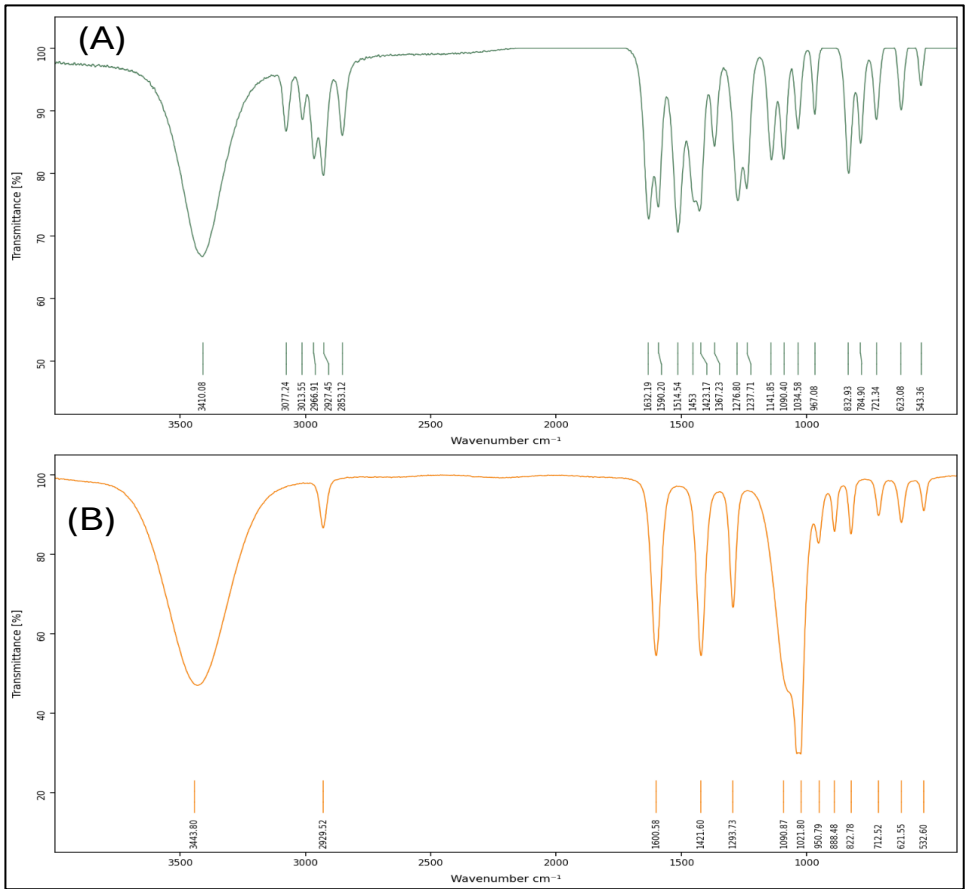

Figure 3: FTIR Spectra of (A) SAE and (B) Physical Mixture

Evaluation of *Syzygium aromaticum* Microspheres (SAMS)

The evaluation of *SAMS* formulations revealed percentage yield ranging from 68.45±2.14% (F1) to 88.65±3.45% (F9), with higher yields observed at increased sodium alginate concentrations. Mean particle size varied between 299.15±12.82 µm (F1) and 425.22±18.16µm (F9), demonstrating significant influence of formulation variables. Polydispersity index values ranged from 0.298±0.020 to 0.423±0.036, indicating acceptable size distribution uniformity (PDI < 0.5). Zeta potential measurements exhibited negative values ranging from -28.45±1.82 mV to -43.85±2.98 mV, confirming good colloidal stability due to electrostatic repulsion between particles, with values exceeding ±30 mV indicating excellent physical stability.

Table 4: Results of Percentage Yield, Particle Size, Polydispersity Index and Zeta Potential of SAMS

Batch	Percentage Yield (%)	Mean Particle Size (µm)	Polydispersity Index (PDI)	Zeta Potential (mV)
F1	68.45 ± 2.14	299.15 ± 12.82	0.298 ± 0.020	-28.45 ± 1.82
F2	72.18 ± 2.45	312.64 ± 13.25	0.312 ± 0.022	-31.28 ± 2.14
F3	75.82 ± 2.68	368.55 ± 15.68	0.365 ± 0.028	-34.65 ± 2.38
F4	71.35 ± 2.32	361.92 ± 15.42	0.358 ± 0.027	-29.85 ± 1.95
F5	78.96 ± 2.85	362.18 ± 15.42	0.360 ± 0.028	-36.42 ± 2.52
F6	82.45 ± 3.12	361.91 ± 15.40	0.359 ± 0.027	-38.75 ± 2.68
F7	76.28 ± 2.74	361.92 ± 15.42	0.360 ± 0.028	-33.52 ± 2.28
F8	85.32 ± 3.28	425.16 ± 18.15	0.422 ± 0.036	-41.28 ± 2.85
F9	88.65 ± 3.45	425.22 ± 18.16	0.423 ± 0.036	-43.85 ± 2.98
F10	79.82 ± 2.92	368.45 ± 15.68	0.365 ± 0.028	-37.12 ± 2.58
F11	83.15 ± 3.18	379.07 ± 16.18	0.376 ± 0.030	-39.85 ± 2.75

F12	80.48 ± 2.98	361.92 ± 15.42	0.360 ± 0.028	-37.85 ± 2.62
F13	81.72 ± 3.05	388.65 ± 16.58	0.385 ± 0.032	-39.15 ± 2.72
F14	82.95 ± 3.14	378.64 ± 16.15	0.375 ± 0.030	-39.52 ± 2.74
F15	81.38 ± 3.02	399.14 ± 17.02	0.396 ± 0.033	-38.45 ± 2.68
F16	82.18 ± 3.08	369.82 ± 15.75	0.367 ± 0.029	-38.92 ± 2.70
F17	81.85 ± 3.06	364.47 ± 15.52	0.362 ± 0.028	-38.68 ± 2.69

Values are expressed as mean ± S.D. (n=3)

The drug loading and entrapment efficiency of *SAMS* demonstrated considerable variation across formulations. Drug loading ranged from 12.45±0.82% (F1) to 24.95±1.68% (F9), with higher values observed at increased sodium alginate concentrations due to enhanced polymer matrix density. Entrapment efficiency varied between 71.45±2.58% (F1) and 90.84±3.85% (F8), indicating effective extract encapsulation within the alginate matrix. Formulations F8 and F9 exhibited superior entrapment efficiency (>90%), attributed to optimal polymer-to-surfactant ratios and controlled stirring speeds. These findings confirmed successful encapsulation of *Syzygium aromaticum* extract within microsphere formulations, ensuring adequate drug payload for therapeutic applications.

Table 5: Drug Loading and Entrapment Efficiency of SAMS

Batch	Drug Loading (%)	Entrapment Efficiency (%)
F1	12.45 ± 0.82	71.45 ± 2.58
F2	15.82 ± 1.05	74.86 ± 2.82
F3	18.65 ± 1.24	82.16 ± 3.25
F4	14.28 ± 0.95	80.09 ± 3.18
F5	19.42 ± 1.32	80.09 ± 3.18
F6	21.85 ± 1.48	80.09 ± 3.18
F7	17.56 ± 1.18	80.09 ± 3.18
F8	23.28 ± 1.58	90.84 ± 3.85
F9	24.95 ± 1.68	90.16 ± 3.82
F10	20.18 ± 1.38	82.56 ± 3.28
F11	22.45 ± 1.52	82.76 ± 3.30
F12	21.12 ± 1.42	80.09 ± 3.18
F13	22.82 ± 1.54	86.35 ± 3.48
F14	23.18 ± 1.56	83.66 ± 3.35
F15	21.68 ± 1.48	87.15 ± 3.52
F16	22.35 ± 1.52	85.68 ± 3.45
F17	22.05 ± 1.50	82.43 ± 3.28

Values are expressed as mean ± S.D. (n=3)

In vitro Drug Release

The in vitro drug release profile of *SAMS* demonstrated biphasic release kinetics over 12 hours. Initial burst release during the first 2 hours ranged from 22.65±1.25% (F1) to 38.92±2.15% (F9), attributed to surface-associated extract dissolution. Subsequently, sustained release was observed with cumulative drug release at 12 hours varying from 65.82 ± 3.38% (F1) to 92.45±4.78% (F9). Higher sodium alginate concentrations in formulations F8 and F9 achieved maximum release (89.68-92.45%), demonstrating efficient extract diffusion from swollen polymer matrix. The controlled release pattern confirmed successful microsphere formulation for prolonged therapeutic action of *SAE.*

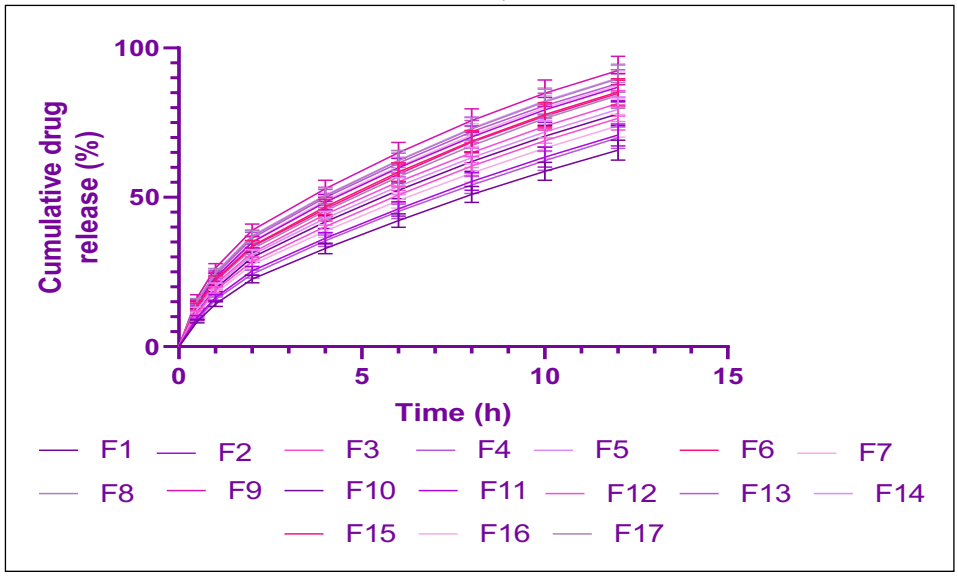

Figure 4: Drug Release Profile of All Batches (F1-F17)

Swelling Index of SAMS

The swelling behavior of *SAMS* exhibited time-dependent water uptake capacity over 12 hours. Initial swelling index at 0.5 hours ranged from 12.45±0.68% (F1) to 28.95±1.58% (F9), progressively increasing to 84.68±4.58% (F1) and 153.15±8.25% (F9) at 12 hours. Formulations with higher sodium alginate concentrations (F8, F9) demonstrated maximum swelling (142.68-153.15%), attributed to enhanced hydrophilic polymer matrix and increased water penetration. The substantial swelling capacity facilitated controlled drug diffusion through the swollen gel network, correlating positively with sustained release profiles and confirming the pH-responsive nature of alginate-based microspheres for effective therapeutic delivery.

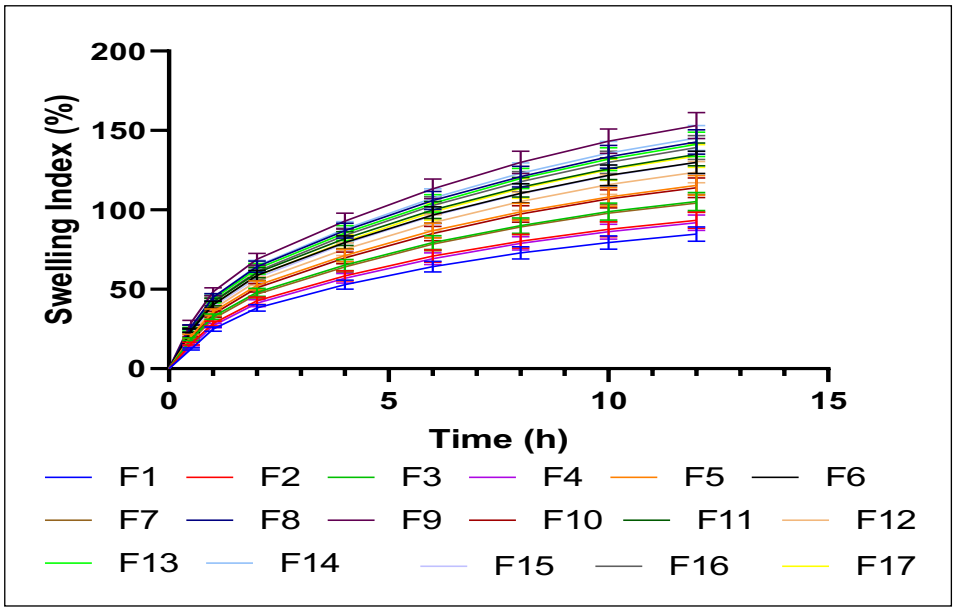

Figure 5: Swelling Index Profile of All Batches (F1-F11)

Optimization of *Syzygium aromaticum* Loaded Microsphere

Effect of Independent Variables on Particle Size

The Box-Behnken Design was employed to optimize formulation parameters affecting particle size of *Syzygium aromaticum* extract-loaded microspheres. Model fit summary analysis revealed that the quadratic model was most appropriate, with high adjusted R^2 of 0.9985 and predicted R^2 of 0.9896 ($p<0.0001$). ANOVA for the quadratic model demonstrated high significance (F-value = 1190.54, $p<0.0001$). Among independent variables, stirring speed exhibited the most profound effect (F-value = 2575.01, $p<0.0001$), followed by sodium alginate concentration (F-value = 1891.98, $p<0.0001$). The interaction term BC (Tween 80 concentration × Stirring speed) showed remarkable significance (F-value = 2932.88, $p<0.0001$). All quadratic terms (A^2, B^2, C^2) demonstrated statistical

significance ($p<0.0001$), with B^2 showing the highest F-value of 1920.65.

The regression equation obtained for particle size optimization was:

Particle Size = 361.97 + 18.8525×A − 4.50125×B − 21.9938×C − 8.8175×AB + 13.8075×AC − 33.195×BC + 5.145×A² + 26.1825×B² − 14.4125×C²

Analysis of polynomial coefficients revealed that sodium alginate concentration (coefficient = +18.8525) positively influenced particle size, while stirring speed (coefficient = −21.9938) demonstrated strong negative effect. The interaction term BC (coefficient = −33.195) showed the most substantial negative effect, suggesting simultaneous increase in Tween 80 concentration and stirring speed significantly reduced particle size. The predicted versus actual plot demonstrated excellent correlation between experimental and predicted values, validating the model's predictive accuracy.

Effect of Independent Variables on Entrapment Efficiency

The optimization of entrapment efficiency was successfully achieved using the quadratic model, with adjusted R^2 of 0.9880 and predicted R^2 of 0.9161 ($p<0.0001$). ANOVA yielded a highly significant F-value of 147.62 ($p<0.0001$). Among independent variables, stirring speed exerted the most significant influence (F-value = 238.08, $p<0.0001$), followed by sodium alginate concentration (F-value = 210.12, $p<0.0001$). Tween 80 concentration also demonstrated significant impact (F-value = 47.73, $p = 0.0002$). The interaction term BC exhibited exceptional significance (F-value = 315.56, $p<0.0001$). Among quadratic terms, B^2 showed the highest significance (F-value = 370.08, $p<0.0001$), while the AB interaction was non-significant ($p = 0.4969$).

The regression equation for entrapment efficiency optimization was:

Entrapment Efficiency = 80.09 + 2.75375×A − 1.3125×B − 2.93125×C − 0.1925×AB + 2.37×AC − 4.7725×BC + 1.48×A² + 5.0375×B² − 1.645×C²

Examination of polynomial coefficients revealed that sodium alginate concentration (coefficient = +2.75375) positively influenced entrapment efficiency, while stirring speed (coefficient = −2.93125) and Tween 80 concentration (coefficient = −1.3125) exhibited negative effects. The interaction term BC (coefficient = −4.7725) demonstrated the most pronounced negative influence. The predicted versus actual plot exhibited excellent agreement between experimental observations and model predictions, confirming the model's robust predictive capability for entrapment efficiency optimization.

Table 6: Model fit summary for particle size and entrapment efficiency

Source	Sequential p-value	Lack of Fit p-value	Adjusted R^2	Predicted R^2	
Particle Size					
Linear	0.0578	< 0.0001	0.2944	-0.1811	
2FI	0.0245	< 0.0001	0.6270	-0.1190	
Quadratic	**< 0.0001**	**< 0.0001**	**0.9985**	**0.9896**	**Suggested**
Cubic	< 0.0001		1.0000		**Aliased**
Entrapment efficiency					
Linear	0.1001		0.2262	-0.2502	
2FI	0.0851		0.4660	-0.4415	
Quadratic	**< 0.0001**		**0.9880**	**0.9161**	**Suggested**
Cubic			1.0000		**Aliased**

Table 7: ANOVA summary for quadratic model for particle size and entrapment efficiency

Source	Sum of Squares	df	Mean Square	F-value	p-value	
Particle Size						
Model	16102.62	9	1789.18	1190.54	<0.0001	significant
A-Sodium Alginate	2843.33	1	2843.33	1891.98	<0.0001	
B-Tween 80	162.09	1	162.09	107.86	<0.0001	
C-Stirring Speed	3869.80	1	3869.80	2575.01	<0.0001	
AB	310.99	1	310.99	206.94	<0.0001	
AC	762.59	1	762.59	507.43	<0.0001	
BC	4407.63	1	4407.63	2932.88	<0.0001	
A^2	111.46	1	111.46	74.16	<0.0001	
B^2	2886.41	1	2886.41	1920.65	<0.0001	
C^2	874.61	1	874.61	581.98	<0.0001	
Residual	10.52	7	1.50			
Lack of Fit	10.46	3	3.49	252.77	<0.0001	significant
Pure Error	0.0552	4	0.0138			
Cor Total	16113.14	16				
Entrapment Efficiency						

Model	383.58	9	42.62	147.62	<0.0001	significant
A-Sodium Alginate	60.67	1	60.67	210.12	<0.0001	
B-Tween 80	13.78	1	13.78	47.73	0.0002	
C-Stirring Speed	68.74	1	68.74	238.08	<0.0001	
AB	0.1482	1	0.1482	0.5134	0.4969	
AC	22.47	1	22.47	77.82	<0.0001	
BC	91.11	1	91.11	315.56	<0.0001	
A^2	9.22	1	9.22	31.94	0.0008	
B^2	106.85	1	106.85	370.08	<0.0001	
C^2	11.39	1	11.39	39.46	0.0004	
Residual	2.02	7	0.2887			
Lack of Fit	2.02	3	0.6737			
Pure Error	0.0000	4	0.0000			
Cor Total	385.61	16				

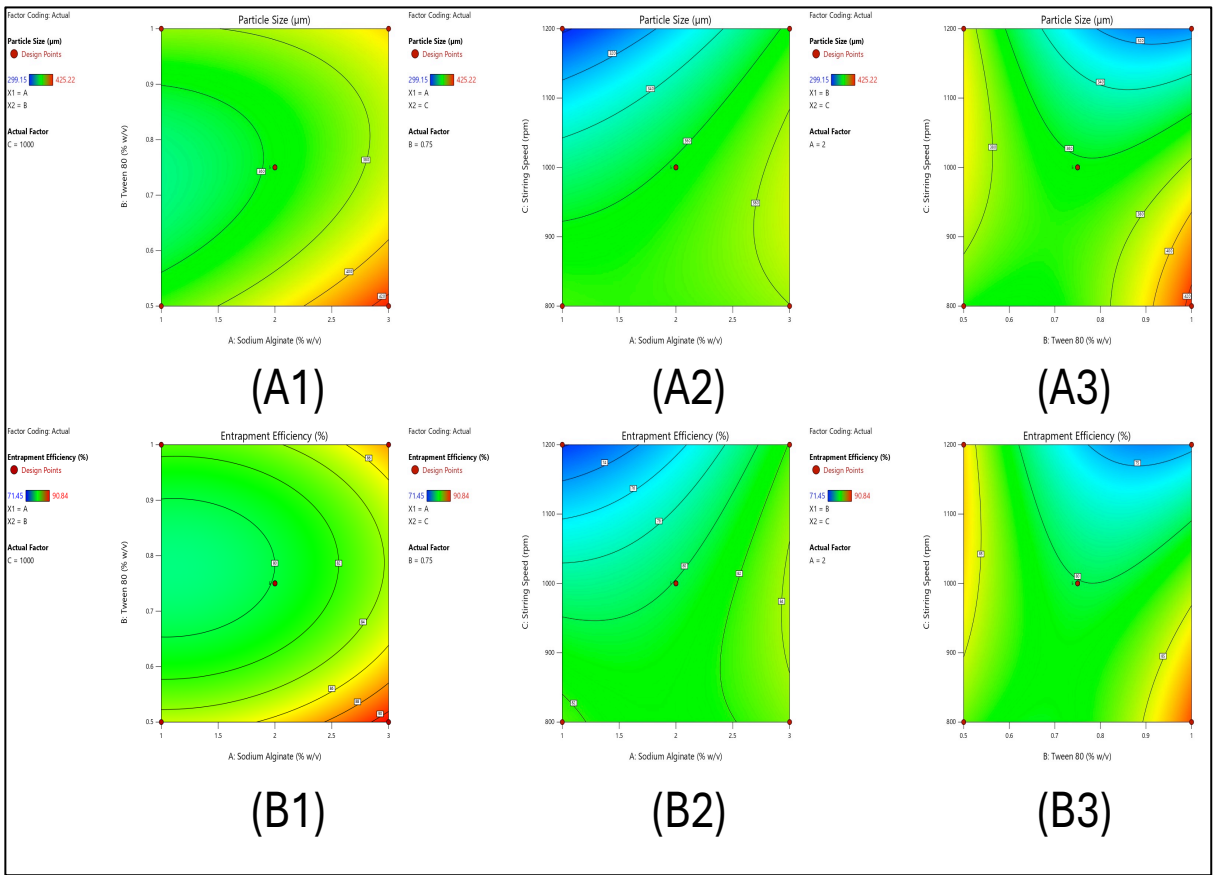

Figure 6: Contour plots showing the effect of formulation variables on (a1-a3) particle size and (b1-b3) entrapment efficiency of *Syzygium aromaticum* extract-loaded microspheres. (a1, b1) Effect of sodium alginate concentration and Tween 80 concentration at constant stirring speed; (a2, b2) Effect of sodium alginate concentration and stirring speed at constant Tween 80 concentration; (a3, b3) Effect of Tween 80 concentration and stirring speed at constant sodium alginate concentration. Green zones indicate optimal ranges, while yellow-to-red zones indicate less desirable values.

Validation of Statistical Model

The optimized formulation (F14) exhibited excellent agreement between predicted and experimental values, with particle size showing 4.79% relative error (predicted: 361.33 µm, practical: 378.64 µm) and entrapment efficiency demonstrating minimal deviation of 0.23% (predicted: 83.85%, practical: 83.66%). These results validated the quadratic model's predictive accuracy.

Table 8: Validation of Optimized Formulation of SAMS

Batch	Response	Predicted value	Practical value	% Relative error
F14	Particle Size	361.33	378.64	4.79

	Entrapment Efficiency	83.85	83.66	0.23

SEM Analysis

The SEM analysis of optimized SAMS (Batch F14) revealed distinct spherical morphology with relatively smooth surface texture and uniform particle distribution at 400× magnification. The micrograph confirmed successful microsphere formation through emulsion-solvent evaporation method, with particles exhibiting characteristic spherical geometry ranging from smaller to larger sizes, consistent with the polydispersity index of 0.375±0.030. The well-separated particles without significant agglomeration demonstrated good dispersibility and confirmed the effectiveness of Tween 80 as emulsifying agent. The smooth surface texture indicated complete solvent evaporation and proper cross-linking with calcium chloride, validating the formulation strategy employed for pharmaceutical application.

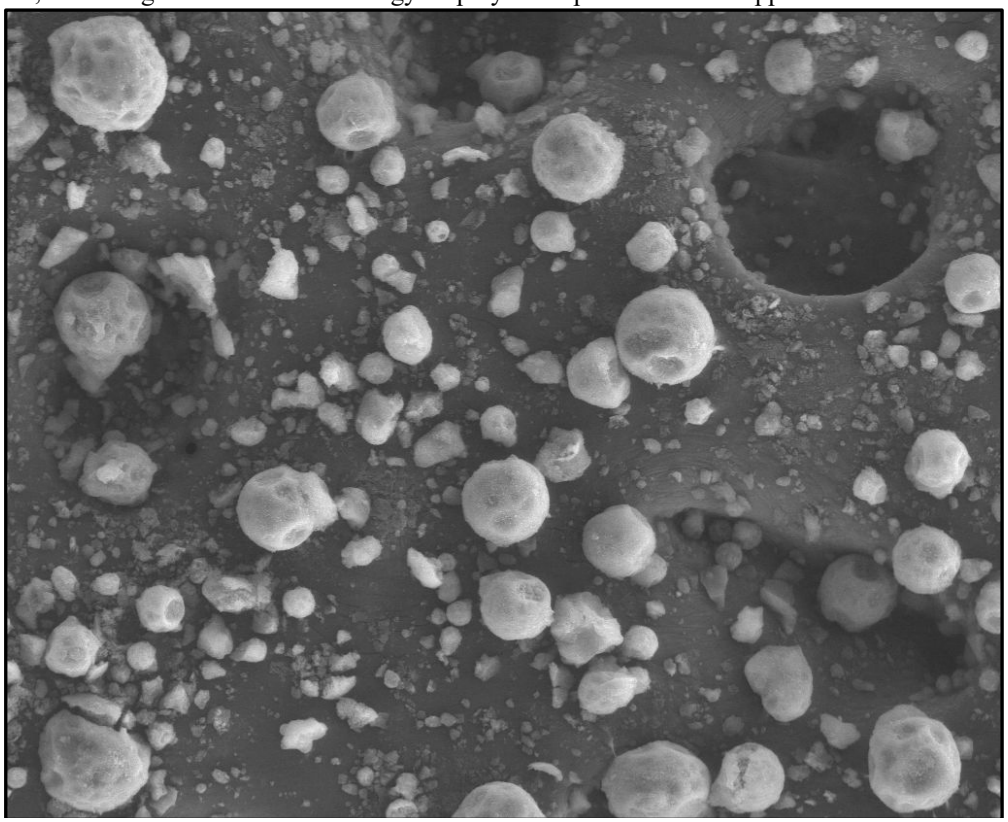

Figure 7: SEM analysis of batch-F14

Stability Study

The stability study of optimized batch F14 demonstrated satisfactory storage stability over six months at both room temperature (25±2°C/ 60±5% RH) and accelerated conditions (40±2°C/ 75±5% RH). At room temperature, minimal deviations were observed in particle size (0.95%), drug content (1.77%), and entrapment efficiency (1.77%). Under accelerated conditions, slightly higher deviations occurred in particle size (2.59%), drug content (4.07%), and entrapment efficiency (4.52%), remaining within acceptable limits (<5%). Physical appearance remained unchanged throughout the study, confirming formulation stability and suitability for pharmaceutical application.

Table 9: Stability Study of Optimized Batch F14 of SAMS at Different Storage Conditions

Time Period (Months)	Physical Appearance	Particle Size (µm)	% Deviation	Drug Content (%)	% Deviation	Entrapment Efficiency (%)	% Deviation
Room Temperature (25±2°C/ 60±5% RH)							
0 (Initial)	Free-flowing, spherical, brown	378.64 ± 16.15	-	99.28 ± 1.32	-	83.66 ± 3.35	-
1	Free-flowing, spherical, brown	379.12 ± 16.22	0.13	99.06 ± 1.36	0.22	83.48 ± 3.38	0.22

2	Free-flowing, spherical, brown	379.82 ± 16.35	0.31	98.76 ± 1.42	0.52	83.18 ± 3.42	0.57
3	Free-flowing, spherical, brown	380.58 ± 16.48	0.51	98.38 ± 1.48	0.91	82.86 ± 3.46	0.96
6	Free-flowing, spherical, brown	382.24 ± 16.72	0.95	97.52 ± 1.62	1.77	82.18 ± 3.56	1.77
Accelerated Condition (40±2°C/ 75±5% RH)							
0 (Initial)	Free-flowing, spherical, brown	378.64 ± 16.15	-	99.28 ± 1.32	-	83.66 ± 3.35	-
1	Free-flowing, spherical, brown	380.26 ± 16.38	0.43	98.74 ± 1.38	0.54	83.06 ± 3.42	0.72
2	Free-flowing, spherical, brown	382.15 ± 16.65	0.93	97.92 ± 1.48	1.37	82.38 ± 3.52	1.53
3	Free-flowing, spherical, brown	384.28 ± 16.95	1.49	96.86 ± 1.62	2.44	81.52 ± 3.64	2.56
6	Free-flowing, spherical, brown	388.45 ± 17.48	2.59	95.24 ± 1.82	4.07	79.88 ± 3.85	4.52

Values are expressed as mean ± S.D. (n=3)

Neuroprotective Activity

The neuroprotective efficacy of *Syzygium aromaticum* extract (SAE) and microsphere formulation (SAMS) was evaluated using rotenone-induced Parkinson's disease model. Rotenone administration (G2) significantly impaired motor coordination, cataleptic behavior, and locomotor activity compared to normal control (G1) ($p<0.05$). SAMS treatment (G4) demonstrated superior therapeutic efficacy compared to SAE (G3), significantly improving rotarod performance (144.3±13.9 sec), reducing catalepsy (33.8±5.9 sec), increasing square crossings (32.5±6.2), rearing frequency (9.7±1.0), and actophotometer counts (146.5±12.8) ($p<0.05$-0.001 vs. SAE). Biochemical analysis revealed SAMS significantly restored antioxidant enzyme levels including catalase (11.25±1.3 µMole/mg protein/min), GSH (10.95±1.3 nM/mg protein), and SOD (6.97±1.1 U/mg protein) while reducing lipid peroxidation (6.65±1.0 nM MDA/g tissue) ($p<0.05$-0.001), demonstrating enhanced neuroprotection through improved bioavailability and sustained release characteristics of the microsphere formulation.

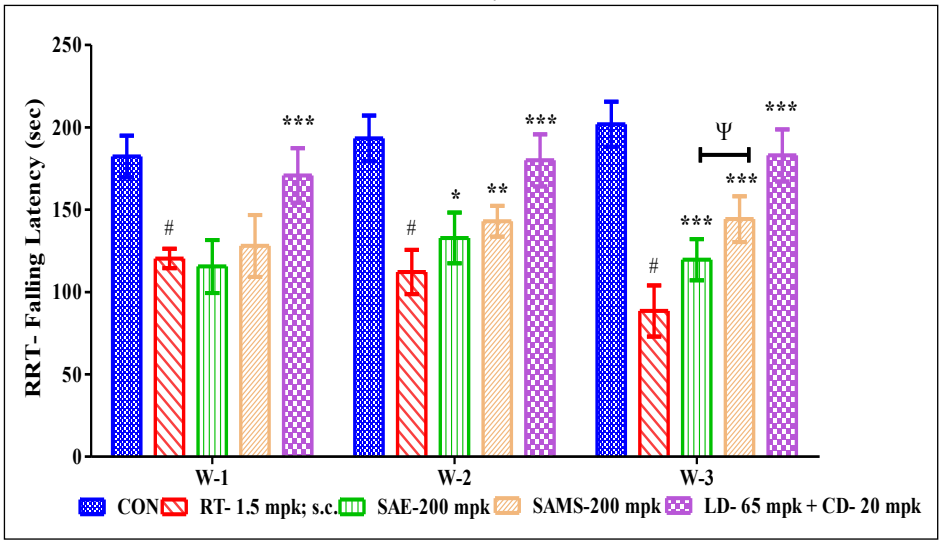

Figure 8: Effect of SAE and SAMS on Rota Rod Test. Values of *p<0.05, **p<0.01, and ***p<0.001 were considered significantly different compared with the disease control group. Values of #p<0.05 indicate significant differences compared with the normal control group, while Ψp<0.05 denotes significant differences compared with the SAE-treated group.

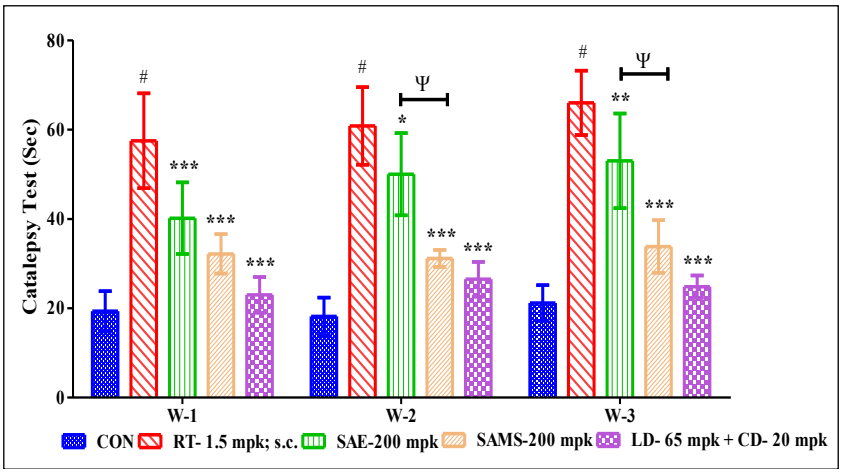

Figure 9: Effect of SAE and SAMS on Catalepsy Test. Values of *p<0.05, **p<0.01, and ***p<0.001 were considered significantly different compared with the disease control group. Values of #p<0.05 indicate significant differences compared with the normal control group, while Ψp<0.05 denotes significant differences compared with the SAE-treated group.

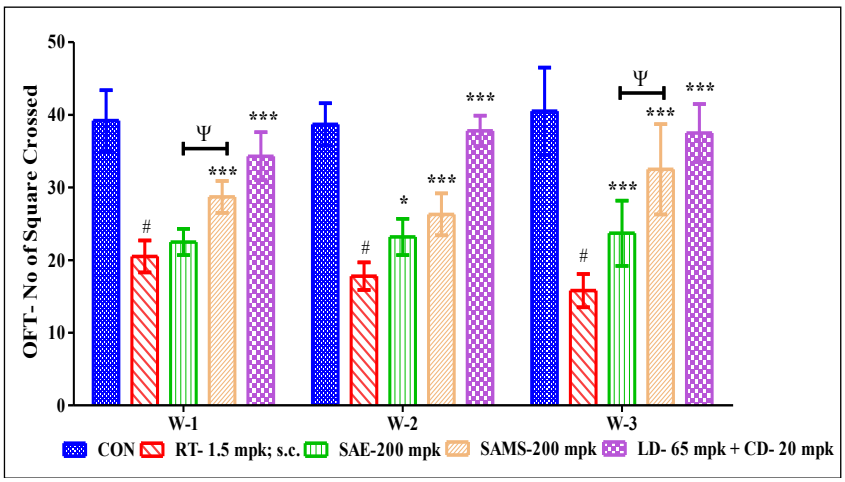

Figure 10-A: Effect of SAE and SAMS on Open Field Test- No of Square Crossed. Values of *p<0.05, **p<0.01, and ***p<0.001 were considered significantly different compared with the disease control group. Values of #p<0.05 indicate

significant differences compared with the normal control group, while Ψp<0.05 denotes significant differences compared with the SAE-treated group.

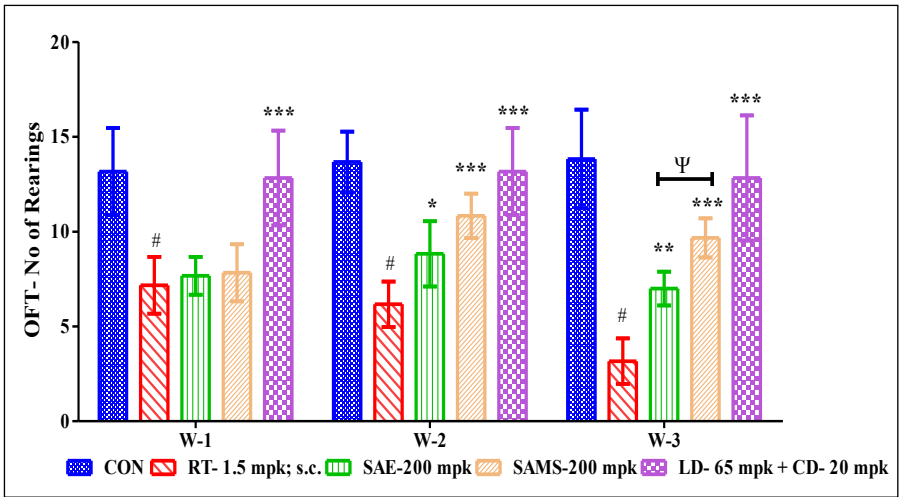

Figure 10-B: Effect of SAE and SAMS on Open Field Test- No of Rearings. Values of *p<0.05, **p<0.01, and ***p<0.001 were considered significantly different compared with the disease control group. Values of #p<0.05 indicate significant differences compared with the normal control group, while Ψp<0.05 denotes significant differences compared with the SAE-treated group.

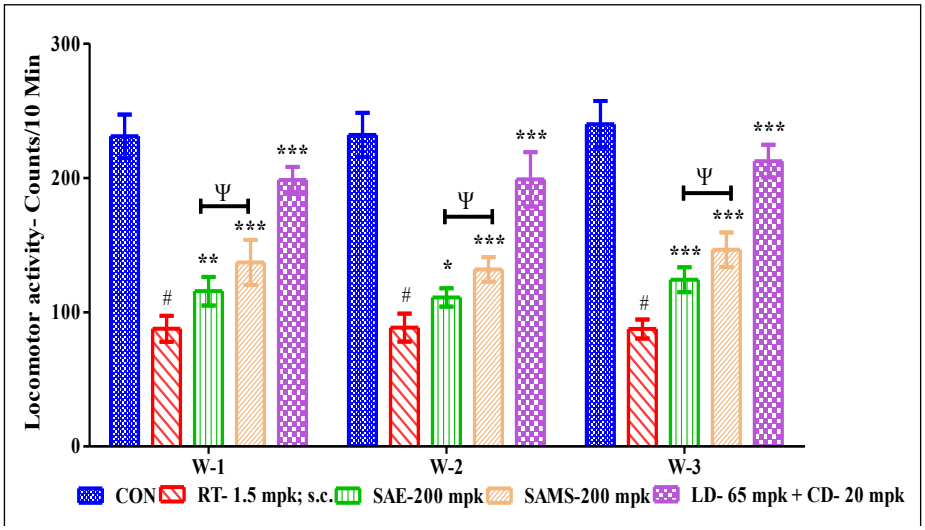

Figure 11: Effect of SAE and SAMS on Actophotometer Test. Values of *p<0.05, **p<0.01, and ***p<0.001 were considered significantly different compared with the disease control group. Values of #p<0.05 indicate significant differences compared with the normal control group, while Ψp<0.05 denotes significant differences compared with the SAE-treated group.

Biochemical Parameters- Antioxidant components

Table 10: Effect of SAE and SAMS on antioxidant components

Groups	Treatment	Catalase activity (µM of H_2O_2 decomposed /mg protein/min)	GSH Level (nM/mg protein)	SOD Level (U/mg Protein)	LPO activity (nM of MDA/ g tissue)
G1	Control	16.10±1.9	15.28±2.4	8.03±1.4	2.51±0.9
G2	RT- 1.5 mpk; s.c.	4.80±1.0#	5.08±0.7#	3.37±0.4#	10.60±1.5#
G3	SAE- 200 mpk	7.85±1.2*	7.98±1.4*	5.02±1.0*	8.50±0.7*
G4	SAMS- 200 mpk	11.25±1.3***Ψ	10.95±1.3*** Ψ	6.97±1.1*** Ψ	6.65±1.0*** Ψ
G5	STD- LD- 65 mpk + CD- 20 mpk	13.10±2.5***	13.62±2.0***	7.73±0.5***	4.75±0.8***

DISCUSSION

The present study successfully developed and optimized *Syzygium aromaticum* extract-loaded microspheres (SAMS) using the Box–Behnken design and comprehensively evaluated their neuroprotective effects in a rotenone-induced model of Parkinson's disease. *Syzygium aromaticum* extract (SAE) was prepared using Soxhlet extraction with an acceptable yield, and its physicochemical characterization was performed to determine fundamental properties essential for formulation development.[43] The calibration curve demonstrated excellent linearity at the maximum wavelength, providing a reliable method for extract quantification throughout the study. Solubility studies indicated that the extract possesses lipophilic characteristics, showing higher solubility in organic solvents such as ethanol and methanol, while exhibiting limited solubility in aqueous media, thereby justifying the need for microencapsulation. The melting point determination suggested the semi-solid nature of the eugenol content, which was further supported by DSC and FTIR analyses.[44]

The optimization strategy employed a Box–Behnken design, in which sodium alginate concentration, Tween 80 concentration, and stirring speed were used as independent variables, while particle size and entrapment efficiency were selected as dependent responses. Statistical analysis demonstrated that both responses were highly significant when fitted to a quadratic model. Among the variables, stirring speed exerted the most significant influence on both responses, followed by sodium alginate concentration.[45] The interaction between Tween 80 concentration and stirring speed was found to be statistically significant, indicating a synergistic effect on formulation characteristics. Analysis of the polynomial equations revealed that sodium alginate concentration had a positive effect on both particle size and entrapment efficiency, whereas stirring speed exhibited a negative effect, with increased stirring speed resulting in smaller particle size and improved drug encapsulation. The optimization process identified formulation F14 as the optimal batch, which was subsequently validated and further characterized.[46]

The optimized formulation F14 exhibited desirable physicochemical properties, including uniform particle size distribution with an acceptable polydispersity index. The zeta potential measurement confirmed excellent colloidal stability, likely due to electrostatic repulsion mechanisms. Drug loading and entrapment efficiency results demonstrated successful encapsulation of SAE within the alginate polymeric matrix. The in vitro drug release profile exhibited biphasic kinetics, characterized by an initial burst release followed by sustained release over time.[47] This controlled release pattern was attributed to the cross-linked alginate network structure, which facilitated the gradual diffusion of the encapsulated extract. Swelling studies revealed time-dependent water uptake capacity, which positively correlated with sustained drug release.[48] Scanning electron microscopy confirmed a spherical morphology with a smooth surface texture, while transmission electron microscopy revealed the characteristic cross-linked polymeric architecture essential for efficient drug loading and controlled release. Stability studies conducted according to ICH guidelines demonstrated satisfactory storage stability, with minimal variations in particle size, drug content, and entrapment efficiency under both room temperature and accelerated conditions.[49]

The neuroprotective efficacy evaluation in rotenone-induced Parkinson's disease model provided compelling evidence for the therapeutic potential of the developed microsphere formulation. Rotenone administration significantly impaired motor functions, as evidenced by reduced rotarod performance, increased cataleptic behavior, and decreased locomotor activity compared to normal control animals.[50] Treatment with SAMS demonstrated significantly superior therapeutic outcomes compared to the pure extract (SAE) across all behavioral parameters. The SAMS-treated animals exhibited marked improvement in motor coordination, with significantly higher falling latency compared to the extract-treated group. Similarly, cataleptic latency was substantially reduced in the microsphere-treated group, approaching near-normal values. Locomotor activity assessments using the open field test and actophotometer revealed significant restoration of ambulatory behavior, with the SAMS group showing markedly better performance than SAE.[51]

Biochemical analysis of brain homogenates revealed profound neuroprotective mechanisms underlying the observed behavioral improvements. SAMS treatment significantly restored antioxidant defense systems, with catalase, GSH, and SOD activities substantially elevated compared to the disease control group. Concurrently, the lipid peroxidation marker MDA was significantly reduced, indicating attenuation of oxidative stress-induced neuronal damage.[52] The superior efficacy of SAMS over the pure extract was attributed to enhanced bioavailability, prolonged circulation time, improved blood–brain barrier penetration, and sustained release characteristics of the microsphere formulation. These findings demonstrate that SAMS represent a promising therapeutic strategy for neurodegenerative disorders, offering improved pharmacokinetic profiles and enhanced neuroprotective efficacy compared to conventional extract administration.[53]

CONCLUSION

The present investigation successfully designed and optimized Syzygium aromaticum extract-loaded microspheres using a Box–Behnken design, achieving optimal formulation characteristics, including a particle size of 378.64 μm, an entrapment efficiency of 83.66%, and drug release of 89.92% at 12 hours. Comprehensive *in vivo* evaluation in a rotenone-induced Parkinson's disease model demonstrated superior neuroprotective effects of the microsphere formulation (SAMS) compared to the pure extract (SAE). The formulation significantly improved motor coordination, reduced catalepsy, enhanced locomotor activity, and restored antioxidant defense systems, as evidenced by increased catalase, GSH, and SOD levels

along with reduced lipid peroxidation. The enhanced therapeutic outcomes may be attributed to improved bioavailability, better blood–brain barrier penetration, and sustained release properties of the formulation, making it a promising therapeutic candidate for the management of neurodegenerative disorders. These encouraging findings warrant further preclinical toxicity studies and clinical trials to evaluate safety and therapeutic efficacy in humans, facilitating the translation of this formulation into a viable neuroprotective therapy.

ACKNOWLEDGEMENTS
The authors extend their sincere gratitude to the Department of Pharmaceutical Sciences, Jayoti Vidyapeeth Women's University, Jaipur–303122, Rajasthan, India, for providing the necessary research facilities to carry out this work.

CONFLICT OF INTEREST
The authors declare no conflict of interest

FINANCIAL ASSISTANCE
This research work was not supported with financial assistance from any funding agencies.

AUTHOR CONTRIBUTION
V.D.- Conceptualization, methodology, investigation, and writing— original draft. S.K.- Conceptualization, data curation, formal analysis, validation, and writing—review and editing. All authors have read and approved the final manuscript and agree to be accountable for all aspects of the work.

ABBREVIATIONS
ANOVA: Analysis of Variance; BBD: Box-Behnken Design; CAT: Catalase; CCSEA: Committee for the Control and Supervision of Experiments on Animals; DMSO: Dimethyl Sulfoxide; DSC: Differential Scanning Calorimetry; EE: Entrapment Efficiency; FTIR: Fourier Transform Infrared Spectroscopy; GSH: Reduced Glutathione; IAEC: Institutional Animal Ethical Committee; ICH: International Council for Harmonisation; MDA: Malondialdehyde; PBS: Phosphate Buffered Saline; PDI: Polydispersity Index; RH: Relative Humidity; SAE: *Syzygium aromaticum* Extract; SAMS: *Syzygium aromaticum* Microsphere Formulation; SEM: Scanning Electron Microscopy; SOD: Superoxide Dismutase; TGA: Thermogravimetric Analysis; UV-Vis: Ultraviolet-Visible Spectroscopy; XRD: X-Ray Diffraction

REFERENCE
1. Wang S, Jiang Y, Yang A, Meng F, Zhang J. The Expanding Burden of Neurodegenerative Diseases: An Unmet Medical and Social Need. Aging and Disease. 2024;16:2937-2952. DOI: 10.14336/ AD. 2024.1071.
2. James LM, Georgopoulos AP. High Correlations Among Worldwide Prevalences of Dementias, Parkinson's Disease, Multiple Sclerosis, and Motor Neuron Diseases Indicate Common Causative Fac tors. Neuroscience Insights. 2022;17:263 31 055221117598. DOI: 10.1177/2 63310552 211 17598.
3. Oyovwi MO, Babawale KH, Jeroh E, Ben-Azu B. Exploring the role of neuromodulation in neurodegenerative disorders: Insights from Alzheimer's and Parkinson's diseases. Brain Disorders. 2025;17:100187. DOI: 10.1016/j.dscb.2025.100187.
4. Ayeni EA, Aldossary AM, Ayejoto DA, Gbadegesin LA, Alshehri AA, Alfassam HA, et al. Neurodegenerative Diseases: Implications of Environmental and Climatic Influences on Neurotransmitters and Neuronal Hormones Activities. International Journal of Environmental Research and Public Health. 2022;19:12495. DOI: 10.3390/ijerp h191912495.
5. Sargsyan T, Simonyan HM, Stepanyan L, Tsaturyan A, Vicidomini C, Pastore R, et al. Neuroprotective Properties of Clove (Syzygium aromaticum): State of the Art and Future Pharmaceutical Applications for Alzheimer's Disease. Biomolecules. 2025;15:452. DOI: 10.3390/biom15030452.
6. Pandey VK, Srivastava S, Ashish, Dash KK, Singh R, Dar AH, et al. Bioactive properties of clove (Syzygium aromaticum) essential oil nanoemulsion: A comprehensive review. Heliyon. 2024;10:e22437. DOI: 10.1016/j.heliyo n.2023.e22437.
7. Xue Q, Xiang Z, Wang S, Cong Z, Gao P, Liu X. Recent advances in nutritional composition, phytochemistry, bioactive, and potential applications of Syzygium aromaticum L. (Myrtaceae). Frontiers in Nutrition. 2022;9:1002147. DOI: 10.3389/f nut.2022.1002147.
8. Vallet-Regi M, Schuth F, Lozano D, Colilla M, Manzano M. Engineering mesoporous silica nanoparticles for drug delivery: where are we after two decades? Chemical Society Reviews. 2022;51:5365-5451. DOI: 10.1039/D1C S00659B.
9. Dumontel B, Conejo-Rodriguez V, Vallet-Regi M, Manzano M. Natural Biopolymers as Smart Coating Materials of Mesoporous Silica Nanoparticles for Drug Delivery. Pharmaceutics. 2023;15:447. DOI: 10.3390/phar maceutics15020447.
10. Semwal P, Rauf A, Olatunde A, Singh P, Zaky MY, Islam MM, et al. The medicinal chemistry of Urtica dioica L.: from preliminary evidence to clinical studies supporting its neuroprotective activity. Natural Products and Bioprospecting. 2023;13:16. DOI: 10.1007/s13659-023-00380-5.
11. Sun Z, Gu X, Hao T, Liu J, Gao R, Li Y, et al. Intra-articular injection PLGA blends sustained-release microspheres loaded with meloxicam: preparation, optimization, evaluation in vitro and in vivo. Drug Delivery. 2022;29:3317-3327. DOI: 10.1080/1 0717544.2022.2144545.

12. Ahmad S, Alrouji M, Alhajlah S, Alomeir O, Pandey RP, Ashraf MS, et al. Secondary Metabolite Profiling, Antioxidant, Antidiabetic and Neuroprotective Activity of Cestrum nocturnum (Night Scented-Jasmine): Use of In Vitro and In Silico Approach in Determining the Potential Bioactive Compound. Plants. 2023;12:1206. DOI: 10.3390/plants12061206.

13. Su Y, Liu J, Tan S, Liu W, Wang R, Chen C. PLGA sustained-release microspheres loaded with an insoluble small-molecule drug: microfluidic-based preparation, optimization, characterization, and evaluation in vitro and in vivo. Drug Delivery. 2022;29:1437-1446. DOI: 10.1080/107 17544. 2022.2072413.

14. Romero-Marquez JM, Navarro-Hortal MD, Forbes-Hernandez TY, Varela-Lopez A, Puentes JG, Pino-Garcia RD, et al. Exploring the Antioxidant, Neuroprotective, and Anti-Inflammatory Potential of Olive Leaf Extracts from Spain, Portugal, Greece, and Italy. Antioxidants. 2023;12:1538. DOI: 10.3390/antiox12081538.

15. Filaferro M, Codeluppi A, Brighenti V, Cimurri F, Gonzalez-Paramas AM, Santos-Buelga C, et al. Disclosing the Antioxidant and Neuroprotective Activity of an Anthocyanin-Rich Extract from Sweet Cherry (Prunus avium L.) Using In Vitro and In Vivo Models. Antioxidants. 2022;11:211. DOI: 10.3390/antiox11020211.

16. Jordan F, Naylor A, Kelly CA, Howdle SM, Lewis A, Illum L. Sustained release hGH microsphere formulation produced by a novel supercritical fluid technology: In vivo studies. Journal of Controlled Release. 2010;141:153-160. DOI: 10.1016/j.jcon rel.2009.09.013.

17. Cleland JL. Solvent Evaporation Processes for the Production of Controlled Release Biodegradable Microsphere Formulations for Therapeutics and Vaccines. Biotechnology Progress. 1998;14:102-107. DOI: 10.1021/bp970128t.

18. Ungaro F, Biondi M, d'Angelo I, Indolfi L, Quaglia F, Netti PA, et al. Microsphere-integrated collagen scaffolds for tissue engineering: Effect of microsphere formulation and scaffold properties on protein release kinetics. Journal of Controlled Release. 2006;113:128-136. DOI: 10.1016/j.jconr el.2006.04.011.

19. Ma X, Santiago N, Chen YS, Chaudhary K, Milstein SJ, Baughman RA. Stability Study of Drug-loaded Proteinoid Microsphere Formulations during Freeze-drying. Journal of Drug Targeting. 1994;2:9-21. DOI: 10.3109/1061 1869409015889.

20. Ji YB, Lee S, Ju HJ, Kim HE, Noh JH, Choi S, et al. Preparation and evaluation of injectable microsphere formulation for longer sustained release of donepezil. Journal of Controlled Release. 2023;356:43-58. DOI: 10.1016/j .jconrel.2 023.0 2.024.

21. Tuncay M, Calis S, Kas HS, Ercan MT, Peksoy I, Hincal AA. Diclofenac sodium incorporated PLGA (50:50) microspheres: formulation considerations and in vitro/in vivo evaluation. International Journal of Pharmaceutics. 2000;195:179-188. DOI: 10.1 016/S0378-5173(99)00394-4.

22. Shi L, Caulfield MJ, Chern RT, Wilson RA, Sanyal G, Volkin DB. Pharmaceutical and Immunological Evaluation of a Single-Shot Hepatitis B Vaccine Formulated With PLGA Microspheres. Journal of Pharmaceutical Sciences. 2002;91:1019-1035. DOI: 10.1002/jps.10042.

23. Rai SY, Ravikumar P. Development and Evaluation of Microsphere Based Topical Formulation using Design of Experiments. Indian Journal of Pharmaceutical Sciences. 2016;78:182-192. DOI: 10.4172/pharmaceutical-sciences.1000102.

24. Wang HT, Schmitt E, Flanagan DR, Linhardt RJ. Influence of formulation methods on the in vitro controlled release of protein from poly (ester) microspheres. Journal of Controlled Release. 199 1;17:23-31. DOI: 10.1016/0168-3659(91)90127-Y.

25. Liggins RT, Cruz T, Min W, Liang L, Hunter WL, Burt HM. Intra-articular treatment of arthritis with microsphere formulations of paclitaxel: biocompatibility and efficacy determinations in rabbits. Inflammation Research. 2004;53:363-372. DOI: 10.1007/s00011-004-1273-1.

26. Bhavsar MD, Amiji MM. Development of Novel Biodegradable Polymeric Nanoparticles-in-Microsphere Formulation for Local Plasmid DNA Delivery in the Gastrointestinal Tract. AAPS PharmSciTech. 2008;9:288-294. DOI: 10.120 8/s 12249-007-9021-9.

27. Soni ML, Kumar M, Namdeo KP. Sodium alginate microspheres for extending drug release: formulation and in vitro evaluation. International Journal of Drug Delivery. 2010;2:64-68. DOI: 10.5138/ijdd.2010.0975.0215.02013.

28. Gaur PK, Mishra S, Bajpai M. Formulation and evaluation of controlled-release of telmisartan microspheres: In vitro/in vivo study. Journal of Food and Drug Analysis. 2014;22:542-548. DOI: 10.1016/j.jfda.2014.05.001.

29. Mundargi RC, Shelke NB, Rokhade AP, Patil SA, Aminabhavi TM. Formulation and in-vitro evaluation of novel starch-based tableted microspheres for controlled release of ampicillin. Carbohydrate Polymers. 2008;71:42-53. DOI: 10.1016/j.carbpol.2007.05.013.

30. Natarajan V, Krithica N, Madhan B, Sehgal PK. Formulation and Evaluation of Quercetin Polycaprolactone Microspheres for the Treatment of Rheumatoid Arthritis. Journal of Pharmaceutical Sciences. 2011;100:195-205. DOI: 10.1002 /jp s.22266.

31. Mordenti J, Thomsen K, Licko V, Berleau L, Kahn JW, Cuthbertson RA, et al. Intraocular pharmacokinetics and safety of a humanized monoclonal antibody in rabbits after intravitreal administration of a solution or a PLGA microsphere formulation. Toxicological Sciences. 1999;52:101-106. DOI: 10.1093/toxsci/52.1.101.
32. Enriquez GG, Rizvi SA, D'Souza MJ, Do DP. Formulation and evaluation of drug-loaded targeted magnetic microspheres for cancer therapy. International Journal of Nanomedicine. 2013;8:1393-1402. DOI: 10.214 7/IJN.S43479.
33. Kumar P, Sachdeva H, Kalra S, Singh B, Dayal R, Singh G. Oxalis corniculata and Ficus religiosa mitigates rotenone-induced Parkinson's disease in Swiss Albino mice: Mechanistic insights and therapeutic potential. Journal of Applied Pharmaceutical Sciences. 2024;14:253-262. DOI: 10.7324/JAPS.2024.161922.
34. Bhadauriya P, Goyal A, Varshney V. Angiotensin (1-7) attenuates rotenone-induced Parkinsonism via Mas receptor and Nrf2 pathway in rats. Journal of Applied Pharmaceutical Sciences. 2025;15:219-229. DOI: 10.7324/JA PS.2025.247748.
35. Shan HM, Maurer MA, Schwab ME. Four-parameter analysis in modified Rotarod test for detecting minor motor deficits in mice. BMC Biology. 2023;21:177. DOI: 10.1186/s12915-023-01679-y.
36. Nemutlu Samur D, Akcay G, Yildirim S, Ozkan A, Ceker T, Derin N, et al. Vortioxetine ameliorates motor and cognitive impairments in the rotenone-induced Parkinson's disease via targeting TLR-2 mediated neuroinflammation. Neuropharmacology. 2022;208:108977. DOI: 10.1016/j.neuropharm.2022.108977.
37. Balakrishnan R, Tamilselvam K, Sulthana A, Mohankumar T, Manimaran D, Elangovan N. Isolongifolene Attenuates Oxidative Stress and Behavioral Impairment in Rotenone-Induced Rat Model of Parkinson's Disease. International Journal of Nutrition, Pharmacology, Neurological Diseases. 2018;8:53-62. DOI: 10.4103/ijnpnd.ijnpnd_3_18.
38. Rafeeq M, Al-Abbasi FA, Afzal M, Saad Alharbi K, Moglad E, Al-Qahtani SD, et al. Effects of a Rosiridin against Rotenone-induced Rats Model of Parkinson's Disease: In-vivo Study and in silico Molecular Modeling. Current Neuropharmacology. 2025;23:1095-1118. DOI: 10.2174/011570159 X349553250126050134.
39. Akshayraj Vanrajbhai C, Thorat VM, Patel VS, Patil KP, Chawla LL. Evaluation of Anxiolytic Activity of Angiotensin Receptor Blockers Using Actophotometer Test in Wistar Rats. Cureus. 2024;16:e69798. DOI: 10.7759/cureus.69798.
40. Garabadu D, Agrawal N. Naringin Exhibits Neuroprotection Against Rotenone-Induced Neurotoxicity in Experimental Rodents. NeuroMo lecular Medicine. 2020;22:314-330. DOI: 10.1007/s12017-019-08590-2.
41. Stepanichev M, Aniol V, Lazareva N, Gulyaeva N. Decreased Hippocampal Neurogenesis in Aged Male Wistar Rats Is Not Associated with Memory Acquisition in a Water Maze. International Journal of Molecular Sciences. 2023;24:13276. DOI: 10.3390/ijms241713276.
42. Bin-Jumah MN, Gilani SJ, Alabbasi AF, Al-Abbasi FA, AlGhamdi SA, Alshehri OY, et al. Protective Effect of Fustin against Huntington's Disease in 3-Nitropropionic Treated Rats via Downregulation of Oxidative Stress and Alteration in Neurotransmitters and Brain-Derived Neurotrophic Factor Activity. Biomedicines. 2022;10:3021. DOI: 10.3390 /biomedicines10123021.
43. Dubey RR, Parikh RH. Two-stage optimization process for formulation of chitosan microspheres. AAPS PharmSciTech. 2009;5:5. DOI: 10.1208/pt050105.
44. Cleland JL, Johnson OL, Putney S, Jones AJS. Recombinant human growth hormone poly(lactic-co-glycolic acid) microsphere formulation development. Advanced Drug Delivery Reviews. 1997;28:71-84. DOI: 10.1016/S0169-409X(97)00051-3.
45. Srivastava AK, Ridhurkar DN, Wadhwa S. Floating microspheres of cimetidine: Formulation, characterization and in vitro evaluation. Acta Pharmaceutica. 2005;55:277-285.
46. Ramazani F, Chen W, Van Nostrum CF, Storm G, Kiessling F, Lammers T, et al. Formulation and characterization of microspheres loaded with imatinib for sustained delivery. International Journal of Pharmaceutics. 2015;482:123-130. DOI: 10.1016/j.ijpharm.2015.01.043.
47. De Souza Nascimento T, Oliveira AV, De Oliveira Belem M, Bezerra JR, Do Carmo MRS, Da Silva ME, et al. The Rotenone-Induced Sporadic Parkinsonism Model: Timeline of Motor and Non-Motor Features. European Journal of Neuroscience. 2025;61:e16669. DOI: 10.1111/ejn.16669.
48. Testa CM, Sherer TB, Greenamyre JT. Rotenone induces oxidative stress and dopaminergic neuron damage in organotypic substantia nigra cultures. Molecular Brain Research. 2005;134:109-118. DOI: 10.1016/j.mo lbrainres.2004.11.007.
49. Rocha SM, Bantle CM, Aboellail T, Chatterjee D, Smeyne RJ, Tjalkens RB. Rotenone induces regionally distinct alpha-synuclein protein aggregation and activation of glia prior to loss of dopaminergic neurons in C57Bl/6 mice. Neurobiology of Disease. 2022;167:105685. DOI: 10.1016/j.nbd.2022.105685.
50. Alam M, Mayerhofer A, Schmidt WJ. The neurobehavioral changes induced by bilateral rotenone lesion in medial forebrain bundle of rats are reversed by L-DOPA. Behavioural Brain Research. 2004;151:117-124.

DOI: 10.1016/j. bbr.2003.08.014.
51. Nicola MA, Attaai AH, Abdel-Raheem MH, Mohammed AF, Abu-Elhassan YF. Neuroprotective effects of rutin against cuprizone-induced multiple sclerosis in mice. Inflammopharmacology. 2024;32:1295-1315. DOI: 10.1007/s 10787-024-01442-x.
52. Pal R, Monroe TO, Palmieri M, Sardiello M, Rodney GG. Rotenone induces neurotoxicity through Rac1-dependent activation of NADPH oxidase in SHSY-5Y cells. FEBS Letters. 2014;588:472-481. DOI: 10.1016/j.febslet.2013.12.011.
53. Dias V, Junn E, Mouradian MM. The Role of Oxidative Stress in Parkinson's Disease. Journal of Parkinson's Disease. 2013;3:461-491. DOI: 10.3233/JPD-130230.